LII Zakopane School of Physics, International Symposium Breaking Frontiers, Zakopane, Poland, May 22–27, 2017

Electrochemical Characterization of $Ca_{65}Mg_{15}Zn_{20}$ Amorphous Alloy in Selected Physiological Fluids

R. Babilas*, D. Szyba, A. Kania, W. Pilarczyk and R. Nowosielski
Institute of Engineering Materials and Biomaterials, Silesian University of Technology,
S. Konarskiego 18a, 44-100 Gliwice, Poland

The corrosion behavior of the bulk glassy samples of $Ca_{65}Mg_{15}Zn_{20}$ alloy was studied by electrochemical measurements and immersion tests in a simulated body fluid, physiological fluid, and the Ringer solution. The results of immersion show that the volume of H_2 evolved after 2 h in simulated body fluid (29.8 ml/cm^2) is the highest in comparison with the results of measurements conducted in physiological fluid (11.3 ml/cm^2) and the Ringer solution (7.4 ml/cm^2). The electrochemical measurements indicated a shift of the corrosion potential (E_{corr}) from –1.58 V for plate tested in a physiological fluid to –1.56 V and –1.54 V for samples immersed in the Ringer solution and simulated body fluid, adequately. The X-ray diffraction measurements were used to determine composition of corrosion products. The corrosion products were mainly identified to be calcium carbonates and calcium/magnesium hydroxides.

DOI: 10.12693/APhysPolA.133.228
PACS/topics: 61.05.cp, 64.70.pe, 68.35.bd, 82.45.Bb, 82.80.Fk

1. Introduction

Recently, a great interest has been aimed to calcium alloys due to their biocompatibility and resorbable properties. Ca–Mg–Zn alloys usually prepared as bulk metallic glasses with amorphous structure can be assumed as potential biomaterials for orthopaedic implants. Ca-based alloys exhibit a low density and do not have negative influence on the human body. However, corrosion resistance of calcium alloys is rather low. Moreover, rapid degradation of these materials in water solutions leads to hydrogen evolution [1–5].

The aim of the work is to study the effect of selected biocorrosive environments on the active behavior of Ca-based bulk metallic glass. The $Ca_{65}Mg_{15}Zn_{20}$ alloy can be expected as the resorbable material due to consisting of the biocompatible elements: Ca, Mg, and Zn.

In this study a simulated body fluid (SBF), physiological fluid (PF) and the Ringer solutions were used. The fluids are often used in many "in vitro" experiments on organs and tissues. The corrosion activity of glassy plates was determined by the hydrogen evolution and potentiodynamic measurements.

2. Experimental

The studies were provided on $Ca_{65}Mg_{15}Zn_{20}$ bulk metallic glasses in the form of plates with a length and a width of 10 mm and a thickness of 1 mm. The ingot of master alloy was prepared by an induction melting of pure elements with purity of 99.9%. The amorphous plates were prepared using the high-pressure die casting, which is a method of the liquid alloy casting into a copper mould [6].

*corresponding author; e-mail: rafal.babilas@polsl.pl

The amorphous structure of the $Ca_{65}Mg_{15}Zn_{20}$ alloy in the form of plates in as-cast state and phase identification after electrochemical measurements was conducted by the X-ray diffraction (XRD) in the reflection mode using Seifert-FPM XRD 7 diffractometer. The Co K_α radiation source was used. The diffraction patterns were collected in the 2Θ range from 30° to 90°.

The glassy state was also verified by using differential scanning calorimetry (DSC) NETZSCH DSC 404C at a constant heating rate of 20 K/min under the argon atmosphere. The DSC method allowed to determine the crystallization temperature and glass-stability of the plates in as-cast state.

The corrosion behavior of the bulk glassy samples was studied by electrochemical measurements and immersion tests at 37 °C in as-prepared SBF, the Baxter PF (5.75 g/dm^3 NaCl, 0.38 g/dm^3 KCl, 0.394 g/dm^3 $CaCl_2 \cdot 6H_2O$, 0.2 g/dm^3 $MgCl_2 \cdot 6H_2O$, 4.62 g/dm^3 $CH_3COONa{\cdot}3H_2O$, 0.9 g/dm^3 $C_6H_5Na_3O_7 \cdot 2H_2O$) and the Baxter Ringer solution (8.6 g/dm^3 NaCl, 0.3 g/dm^3 KCl, 0.48 g/dm^3 $CaCl_2{\cdot}6H_2O$). The SBF was prepared according to a procedure described in [7]. The following reagents for preparing 1000 ml of SBF were used: 8.035 g/dm^3 NaCl, 0.355 g/dm^3 $NaHCO_3$, 0.225 g/dm^3 KCl, 0.231 g/dm^3 $K_2HPO_4 \cdot 3H_2O$, 0.311 g/dm^3 $MgCl_2 \cdot 6H_2O$, 1.2 g/dm^3 1 M HCl, 0.292 g/dm^3 $CaCl_2$, 0.072 g/dm^3 Na_2SO_4, 6.118 g/dm^3 $(HOCH_2)_3CNH_2$.

The potentiodynamic measurements were conducted in a typical three-electrode cell using a sample as working electrode, a saturated calomel electrode (SCE) as reference electrode and a platinum counter electrode in Autolab 302N workstation.

The corrosion behavior was evaluated by recording of the open-circuit potential (E_{OCP}) and potentiodynamic polarisation curves in the potential range E_{OCP} –300 mV

to $E_{OCP}+300$ mV. The corrosion potential (E_{corr}), corrosion current density (j_{corr}) and polarisation resistance (R_p) was also determined by the Tafel extrapolation [8]. The samples were measured from a near-steady-state corrosion potential after a period of open-circuit potential stabilization. The E_{OCP} was monitored from 500 to 3600 s at 37 °C.

The immersion tests at 37 °C were conducted to determine an amount of evolved hydrogen. The immersion time was 120 min. Basing on the experimental set up described in [9], the amount of evolved hydrogen was measured.

3. Results and discussion

The X-ray diffraction pattern of the plates of the as-cast state is presented in Fig. 1 and shows a broad diffraction halo indicating the formation of an amorphous structure. In addition, Fig. 2 presents the experimental DSC curve of as-prepared metallic glass. The onset (T_x), first and second peak crystallization (T_{p1}, T_{p2}) temperatures are determined from the DSC trace. They are found to be 418, 428, and 507 K, adequately.

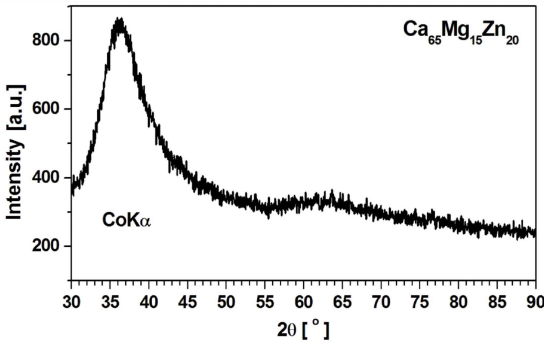

Fig. 1. XRD pattern of $Ca_{65}Mg_{15}Zn_{20}$ alloy in the form of plate with thickness of 1 mm.

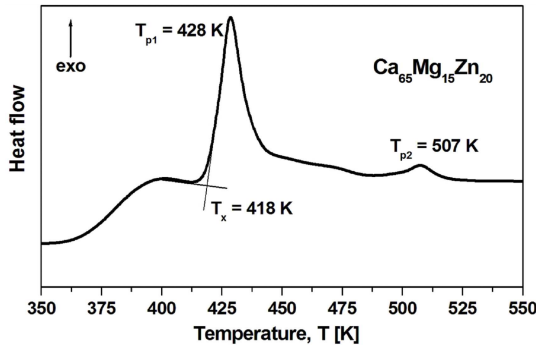

Fig. 2. DSC curve of $Ca_{65}Mg_{15}Zn_{20}$ plate in as-cast state.

The E_{OCP} curves as a function of immersion time for glassy plates treated in SBF, PF and the Ringer solution at 37 °C are shown in Fig. 3. The E_{OCP} trace for sample

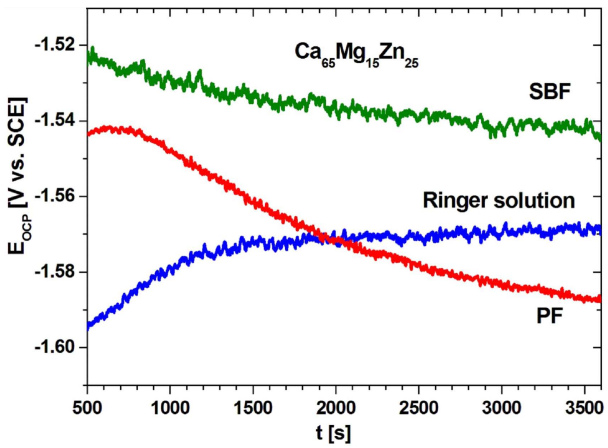

Fig. 3. Variation of the open-circuit potential with time for samples in SBF, PF, and the Ringer solution at 37 °C.

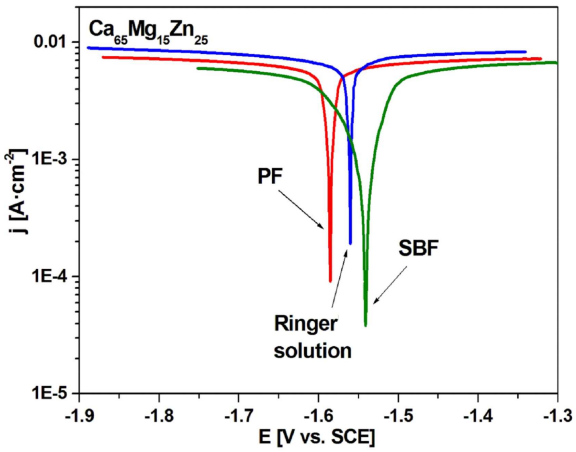

Fig. 4. Polarization curves of studied alloy samples in SBF, PF, and the Ringer solution at 37 °C.

immersed in the Ringer solution exhibits an increasing tendency and shifts towards the positive potential during 3600 s. In the opposite, the E_{OCP} traces for plates treated in SBF and PF show a decreasing behavior. The final values of the E_{OCP} for tested samples of examination in SBF, PF, and the Ringer solution after 3600 s was noticed to be –1.54, –1.57, and –1.59 V vs. SCE, consequently.

TABLE I

The results of corrosion investigations of $Ca_{65}Mg_{15}Zn_{20}$ metallic glasses in SBF, PF, and the Ringer solution (E_{OCP} — open-circuit potential, E_{corr} — corrosion potential, R_p — polarization resistance, j_{corr} — corrosion current density).

Sample	E_{OCP} [V]	E_{corr} [V]	R_p [Ω cm^2]	j_{corr} [mA/cm^2]
SBF	-1.54	-1.54	11.11	5.81
Ringer	-1.57	-1.56	2.20	1.52
PF	-1.59	-1.58	4.34	0.85

The potentiodynamic polarization curves of the samples tested in SBF, PF, and the Ringer solution at 37 °C are shown in Fig. 4. The polarization curves of the samples tested in different biocorrosive solutions present a similar shape, but significant difference in values of corrosion potential can be noticed. The best value of the E_{corr} was obtained for sample examined in SBF medium.

The electrochemical measurements indicated a shift of the corrosion potential from –1.58 V for plate tested in a physiological fluid to –1.56 and –1.54 V for samples immersed in the Ringer solution and SBF, adequately. The j_{corr} of the glassy samples examined in SBF, the Ringer solution, and PF are 5.81, 1.52, and 0.85 mA/cm^2, adequately. The changes of polarization resistance were also detected from 11.11 Ω cm^2 for SBF to 4.34 Ωcm^2 for PF and 2.2 Ω cm^2 evaluated for the Ringer solution. Electrochemical measurements data including the open-circuit potential, corrosion current density, corrosion potential, and polarization resistance are also concluded in Table I.

Nowosielski et al. [10] revealed that the $Ca_{60}Mg_{20}Zn_{20}$ metallic glasses are also reactive in PF and the Ringer solution. However, studied Ca-based samples show better corrosion potential and reduced corrosion activity than $Ca_{65}Mg_{15}Zn_{20}$ alloy tested in SBF, PF, and the Ringer solution at 37 °C. For comparison, the j_{corr} of the $Ca_{60}Mg_{20}Zn_{20}$ glass is 0.86 mA/cm^2 after tests in physiological fluid and 1.03 mA/cm^2 after examinations in the Ringer solution, respectively. The decreased corrosion activity of $Ca_{60}Mg_{20}Zn_{20}$ alloy can be probably related to lower Ca concentration, which is extremely reactive.

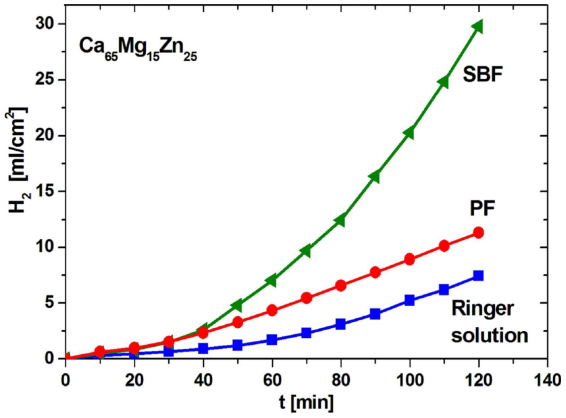

Fig. 5. Hydrogen evolution volume in a function of the immersion time in SBF, PF, and the Ringer solution at 37 °C.

Figure 5 shows the influence of biocorrosion media on the hydrogen evolution volume of $Ca_{65}Mg_{15}Zn_{20}$ glass as a function of time. The results of immersion show that the volume of H_2 evolved after 2 h in SBF (29.8 ml/cm^2) is the highest in comparison with the measurements conducted in PF (11.3 ml/cm^2) and the Ringer solution (7.4 ml/cm^2).

The results of hydrogen evolution indicate that SBF is the most aggressive corrosive medium. The growing tendency of evolved hydrogen as a function of time was also observed for samples examined in all selected fluids.

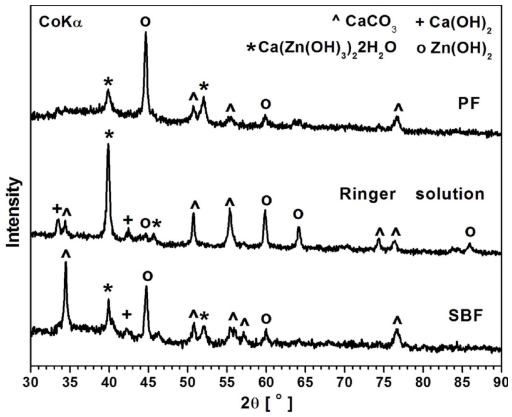

Fig. 6. XRD patterns of the corrosion products after 1 h of electrochemical measurements in SBF, PF, and the Ringer solution at 37 °C.

The XRD analysis (Fig. 6) of the corrosion products formed after 1 h of potentiodynamic tests in SBF, PF, and the Ringer solution showed that the calcium hydroxide ($Ca(OH)_2$), the calcium carbonate ($CaCO_3$), the zinc hydroxide ($Zn(OH)_2$) and the calcium zinc hydroxide hydrate ($Ca(Zn(OH)_3)_2{\cdot}2H_2O$) can be identified.

Based on the XRD results and data presented in [11], the main corrosion reactions in selected fluids (1–6) were listed below

$$Ca + 2H_2O \rightarrow Ca(OH)_2 \downarrow + H_2 \uparrow, \quad (1)$$

$$Ca(OH)_2 + CO_2 \rightarrow CaCO_3 \downarrow + H_2O, \quad (2)$$

$$Mg + 2H_2O \rightarrow Mg(OH)_2 \downarrow + H_2 \uparrow, \quad (3)$$

$$Mg(OH)_2 + CO_2 \rightarrow MgCO_3 \downarrow + H_2O, \quad (4)$$

$$Zn + 2OH^- \rightarrow ZnO \downarrow + H_2O, \quad (5)$$

$$2ZnO + Ca(OH)_2 + 4H_2O \rightarrow Ca(Zn(OH)_3)_2 \cdot 2H_2O. \quad (6)$$

The corrosion mechanism of studied alloy indicated that hydroxides ($Ca(OH)_2$, $Mg(OH)_2$) are formed firstly. Carbonates are also formed ($CaCO_3$, $MgCO_3$). Due to the hydrogen evolution the corrosion layer is going to be porous without protective function. The corrosive solutions react with unprotected metal layer. Nevertheless, hydroxides and oxides (ZnO) could not stop the corrosion degradation and calcium zinc hydroxide hydrates are formed.

Obtained results can be confirmed by results reported by Wang et al. [11] who examined by XRD method the corrosion products of $Ca_{65}Mg_{15}Zn_{20}$ glass after immersion in Hank's solution. The detected phases were mainly composed of calcium phosphate, calcium hydroxide, magnesium hydroxide, zinc hydroxide, calcium zinc hydroxide hydrate. Moreover, Dahlman et al. [12] stated that corrosion products of the same amorphous alloy after tests in distilled water consisted at least three phases: calcium hydroxide, calcium zinc hydroxide hydrate, and calcium zinc.

4. Conclusions

The glassy Ca-based plates as potential orthopaedic implants were investigated in selected biocorrosive fluids. The electrochemical measurements reported a shift of the corrosion potential from –1.58 V for sample examined in a physiological fluid to –1.56 and –1.54 V for samples immersed in the Ringer solution and SBF, adequately.

Only, the E_{OCP} trace for sample immersed in the Ringer solution exhibits increasing tendency and shifts towards the positive potential. The decrease of the open-circuit potential at the end of immersion indicates further dissolution of the samples studied in PF and SBF. The volume of H_2 evolved after 2 h in SBF is the highest in comparison with the results of tests conducted in PF and the Ringer solution.

The XRD analysis of the corrosion products of the samples after 1 h of electrochemical test confirmed a formation of calcium and zinc hydroxides, calcium zinc hydroxide hydrates, and also calcium carbonates.

The corrosion mechanism of studied alloy in the selected biocorrosive fluids is rather the same, but more aggressive environment of SBF makes that the hydrogen evolution is more progressing. The different corrosion behavior of $Ca_{65}Mg_{15}Zn_{20}$ glass in the simulated body fluid is caused by ion concentrations very similar to those of human blood plasma [7]. In this case, PF and the Ringer solution seem to be less suitable for biocorrosion experiments than SBF. What is more, the SBF is useful for predicting the bioactivity of potentially materials. The "in vitro" tests in SPB can be used for evaluating bone bioactive materials before animal testing.

Acknowledgments

The work was partially supported by National Science Centre under research project no. 2013/09/B/ST8/02129.

References

[1] J.Q. Wang, J.Y. Qin, X.N. Gu, Y.F. Zheng, H.Y. Bai, *J. Non-Cryst. Solids* **357**, 1232 (2011).

[2] M. Salahshoor, Y. Guo, *Materials* **5**, 135 (2012).

[3] H.F. Li, X.H. Xie, K. Zhao, Y.B. Wang, Y.F. Zheng, W.H. Wang, L. Qin, *Acta Biomater.* **9**, 8561 (2013).

[4] Y.N. Zhang, G.J. Rocher, B. Briccoli, D. Kevorkov, X.B. Liu, Z. Altounian, M. Medraj, *J. Alloys Comp.* **552**, 88 (2013).

[5] H.F. Li, Y.B. Wang, Y. Cheng, Y.F. Zheng, *Mater. Lett.* **64**, 1462 (2010).

[6] R. Babilas, A. Bajorek, W. Simka, D. Babilas, *Electrochim. Acta* **209**, 632 (2016).

[7] T. Kokubo, H. Takadama, *Biomaterials* **27**, 2907 (2006).

[8] E. McCafferty, *Corros. Sci.* **47**, 3202 (2005).

[9] Z. Shi, A. Atrens, *Corros. Sci.* **53**, 226 (2011).

[10] R. Nowosielski, A. Bajorek, R. Babilas, *J. Non-Cryst. Solids* **447**, 126 (2016).

[11] Y.B. Wang, X.H. Xie, H.F. Li, X.L. Wang, M.Z. Zhao, E.W. Zhang, Y.J. Bai, Y.F. Zheng, L. Qin, *Acta Biomaterials* **7**, 3196 (2011).

[12] J. Dahlman, O.N. Senkov, J.M. Scott, D.B. Miracle, *Mater. Trans.* **48**, 1850 (2007).